Audio Engineering Society
Convention Paper
Presented at the 111th Convention
2001 September 21–24 New York, NY, USA

Modern Development Tools for Dynamic Transducers

Martin Opitz, Richard Barnert
AKG Acoustics GmbH
Lemboeckgasse 21-25
1230 Wien, Austria
OpitzM@akg-acoustics.com, BarnertR@akg-acoustics.com

ABSTRACT

The growing use of multimedia applications in mobile equipment like notebooks, MP3-players or mobile phones causes the need for miniature speakers with optimized performance. In order to improve their acoustic performance the detailed behavior of transducers has to be studied. Modern tools like numeric simulation programs and laservibrometry give a deeper sight into the demanded characteristic features. In this paper the application of three important tools is described, examples are shown.

INTRODUCTION

This paper presents an overview of helpful tools for the design of electrodynamic transducer parameters. Due to the growing demand for smaller and louder transducers – like in the telecom market - these products have to be optimized. Especially when operated at high excursions, nonlinear effects become more and more obvious. Two dominant factors for nonlinear performance of loudspeakers are the magnetic flux density B(z) that varies with the position z of the voice coil and the nonlinear mechanical stiffness of the diaphragm [1]. The well-known electro-acoustic equivalent circuits are not able to consider most of these nonlinearities. The tools presented in this paper turned out to be very powerful for the analysis of nonlinear effects and dynamic parameters. We concentrate on three different tools, namely “Magnetic Field Computations”, “Mechano-Acoustical Computations” and “Optical Measurements”.

MAGNETIC FIELD COMPUTATIONS

The shape and distribution of the magnetic flux density vector is of great importance for the performance of the transducer, especially when operated at high excursions. The following considerations are related to small dynamic loudspeakers, where these large excursions frequently occur. Especially the need for high sound pressure levels results in high excursions of the voice coil. Similar aspects are valid for dynamic microphone transducers.

The permanent magnet generates a magnetic flux that is guided by softmagnetic material. This whole assembly is denoted as magnetic circuit. There are several optimization goals when designing the magnetic field distribution in the magnetic circuit:

- High magnetic flux density B integrated over the voice coil volume on the whole path of the voice coil on its way between the points of inflexion.
- High linearity of the magnetic flux density B integrated over the voice coil volume on the whole path of the voice coil on its way between the points of inflexion.

In order to fulfil these requirements, a number of parameters are available to design the magnetic circuit. One can classify these

parameters into two classes: geometric properties and material properties which are closely related to each other.
Nowadays Neodymium-Iron-Boron magnets are frequently used as permanent magnets in dynamic acoustic transducers. As these magnets show a relative permeability of slightly larger than 1.0 the design of flat transducers is easy to realize. Such a flat design takes full advantage of the maximum possible energy density provided by a neodymium-iron-boron magnet of given mass.

The iron parts of the magnetic circuit guide the magnetic flux to the air gap where the voice coil is moving. The flux density in this volume is of special interest as it has to fulfil the above mentioned criteria of quantity and linearity.

To estimate the properties of the magnetic circuit a number of simulation tools are available. As a producer of dynamic acoustic transducers we started the numerical design of magnetic circuits at a time when the number of commercially available simulation software in this area was very limited. For this reason we decided to develop our own software to compute the distribution of magnetic flux density.

The advantage of such an in-house development lies in the fact that user specific modifications can easily be implemented. An example for such an adaptation will be given below.

The properties of our software for the computation of magnetostatic fields are:

- Simple user interface
- Nonlinear magnetic material properties
- 2D cylindrical symmetry
- Finite Difference solver
- Boundary conditions: free field, external field
- Postprocessing: B-field, H-field, shearing, nonlinear distortion during voice coil movement

Preprocessing Programs

The preprocessor part consists of three programs:

MEV: Input of material properties both for the hardmagnetic materials like permanent magnets and the softmagnetic materials. These softmagnetic materials are characterized by a permeability that depends on the size of the magnetic field strength. In this way nonlinear magnetic properties are included in the iteration process. This means that saturation effects are modeled that occur in certain parts of the magnetic circuit.

BSM: Calculation of a boundary shift matrix. The boundary shift matrix is necessary for the so called free field boundary condition. This means that the user is looking on the model and the appropriate field distribution through a kind of window. The BSM guarantees that this field distribution intersects the boundary as if it would extend to infinity. The program BSM computes the necessary transfer matrix in order to simulate the freefield properties. For details see [2].

MAVA: This is the main preprocessor program. The geometry of the different parts is defined here as well as the kind of material, the direction of magnetization and several numerical parameters like the desired accuracy of the resulting field distribution. Also the frame size is chosen here. The frame size is the outer boundary of the mesh on which the magnetic potential is calculated as described below. Typical values for the frame are 250 mesh points in radial direction and 250 mesh points in axial direction.

Solver Program

MAVB: The solver program is a Finite Difference program that computes the magnetic potential in ampere on a mesh of uniformly distributed field points. This computation is done by an iteration process. At the beginning of this process, an initial potential distribution is estimated, e.g. zero ampere at all mesh points. The iteration algorithm is applied by scanning one mesh point after the other. For every mesh point an improved estimation of the potential is estimated by using the potential at the adjacent mesh points. Forming the gradient of the magnetic potential yields the corresponding magnetostatic field vector.

The condition to break off the iteration is determined by the desired accuracy. In many practical cases this accuracy lies between 1 and 2 percent. This results in an approximate number of iterations between 10000 and 20000. Typical solution times for such a model are approximately 20 minutes on a Pentium II with 300MHz processor speed. During the iteration several parameters are listed on the screen that allow the user to follow the iteration process and the achieved accuracy.

Postprocessing Programs

MAPLOT: This postprocessing program allows the visualization of the magnetic potential by drawing lines of equal potential. Normally this potential has a large gradient in the air gap corresponding to a maximum of magnetic field strength and the magnetic flux density in this area.

SATPLOT: This tool delivers plots of

- the magnetic field
- the magnetic flux density
- the shearing

by drawing areas of different colors characterizing the value of the respective parameters.

AUSW: Special care is given to the evaluation of results in the air gap. In this region the voice coil is moving up and down. Several characteristic values are estimated that describe the quality of the magnetic circuit. One of the most important factors is the **flux efficiency**: This factor compares the magnetic flux that penetrates the voice coil with the total magnetic flux generated by the magnet. The flux efficiency describes the degree of exploitation of the permanent magnet. The goal is to minimize the so called stray flux and to increase the useful flux through the voice coil.

Of special importance is the possibility to determine the flux efficiency factor for different voice coil situations in a postprocessing section without the need to recalculate the whole magnetic potential.

LUFTPLOT: To quantify the effect of large excursions of the voice coil, a postprocessing program was written that determines the **harmonic distortions** of 2nd and 3rd order as well as total harmonic distortions due to the effect that the average flux density in the volume of the voice coil is not constant over the voice coil path. The effective force on the voice coil

$$F(z) = B(z) \cdot l \cdot I$$

changes correspondingly during this movement. In this expression the following parameters are used:

z......... the current voice coil position
B(z).... radial component of the average magnetic flux density effective over the volume of the voice coil, depending on the current voice coil position z
l........ the coil length and
I....... the electric current in the voice coil.

Example

To illustrate the above mentioned tools an example is given for a dynamic transducer used in professional studio headphones. In this application there are high requirements concerning linearity and maximum sound pressure level.

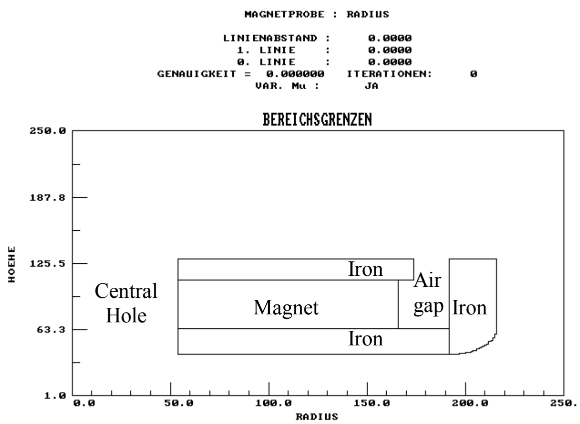

Fig. 1. Cross section of dynamic transducer with permanent magnet and iron parts

Figure 1 shows a cross section view of the geometry of the transducer with cylindrical symmetry. The ordinate axis is the z-direction, the abscissa denotes the radius. The outer diameter of the transducer is 30mm. In figure 1 one can see the permanent magnet (NdFeB type), the iron parts and the air gap in the right upper part of the magnetic circuit. You can see that there is a central hole in the model. Also shown is a curve in the outer lower iron part. The permanent magnet is vertically polarized.

The computation of the magnetic field is done by introducing nonlinear material properties. This is realized by iteratively adapting the relative permeability within the iron parts in dependence of the local magnetic field strength. Results can be obtained with the postprocessing programs as shown in figure 2 to figure 5.

Figure 2 shows a contour plot with lines of equal magnetic potential in Ampere. It can be seen in figure 2 that there is a strong concentration of potential lines in the air gap indicating a maximum of the H-field. The absolute maximum and the absolute minimum of the magnetic potential are located at the top and at the bottom of the ring magnet, where the remanent magnetization M_0 has a discontinuity.

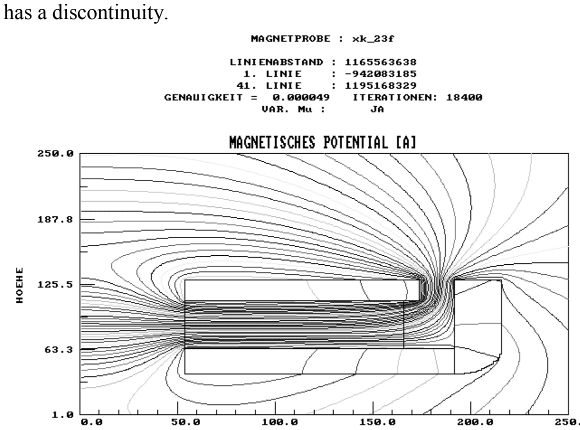

Fig. 2. Lines of equal magnetic potential

In figure 3 the magnetic flux density (absolute value) is shown as texture. A concentration of the magnetic flux density is visible in the iron parts near the air gap. With the help of such plots possible saturation effects in iron parts are revealed. In many applications like for example in mobile phones a flat loudspeaker design is required. On the other hand magnetic saturation effects can easily occur when iron parts of the magnetic circuit are designed too small. In these cases the cross section in the iron parts becomes too small to guide the whole magnetic flux towards the air gap. As a consequence an increased stray field occurs. The higher amount of stray field is described by a lower flux efficiency factor as mentioned above. By evaluating the flux density plots the designer of the magnetic circuit has the possibility to find a compromise between these two contradictory requirements of flat design on the one hand and high magnetic flux density in the air gap on the other hand.

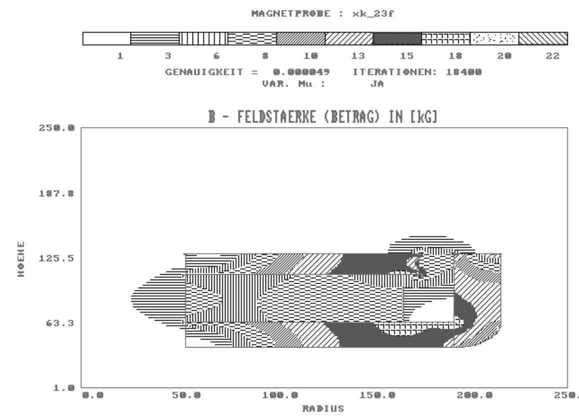

Fig. 3. Magnetic flux density (absolute value)

The situation around the air gap is of special interest, as the electro-mechanical energy conversion occurs here. In figure 4 the radial component of the magnetic flux density in the air gap is plotted as a function of the height z. This radial component is responsible for the effective induction taking place in the voice coil. In figure 4, a movement to the right side corresponds to a movement out of the magnetic circuit, which is shown as an upward movement in figure 3. The different lines in figure 4 represent the flux density (radial component) at different radii. The highest curve in figure 4 is the cross section at the smallest radius in the air gap. The flux density is decreasing below and above the air gap and shows a maximum in the air gap itself. An interesting detail is the focusing effect at the edges of the pole plate: In figure 2 one can see the concentration of the potential lines near these edges which results in an increased flux density to be seen in figure 3 and figure 4. This local flux density increase is not a disturbing factor in real applications because in order to determine the effective force onto the voice coil, the flux density vector has to be integrated over the whole volume of the voice coil.

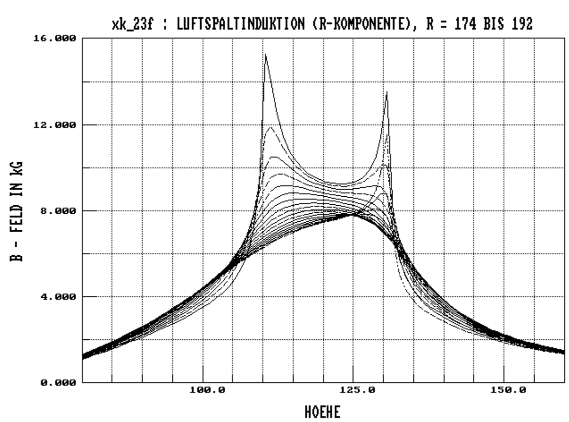

Fig. 4. Radial flux density vector in the air gap as a function of the height coordinate.

In figure 4 it can clearly be seen that the flux density B is not constant neither in radial nor in axial direction. While the radial dependency is not of greater importance, the axial decrease of the flux density is responsible for nonlinear harmonic distortions that occur when the voice coil is moving upwards and downwards in the air gap (corresponding to left-right movement in figure 4). This nonlinear behavior of the flux density component causes harmonic distortions as described in the chapter “Postprocessing Programs”.

In a postprocessing session the voice coil geometry and the amplitude of the voice coil are chosen by the user. It is assumed that a sinusoid electrical input signal with a frequency of 100Hz is applied to the voice coil terminals. The resulting force on the diaphragm can deviate significantly from this sinusoidal course due to the nonlinear flux density component.

In figure 5 an example for such a postprocessing investigation is shown: In the upper right corner the original electrical sinusoid signal is shown for one period as well as the resultant force on the voice coil. One can clearly see significant differences between these two curves.

A quantification of this distortion is achieved by applying a discrete Fourier transform onto this distorted signal. The resultant amplitude spectrum is shown in the lower part of figure 5. One can see the peak at 100Hz corresponding to the main component. The spectrum is normalized so that the amplitude component at 100Hz has a value of zero decibel. In figure 5 harmonic components up to the 50th order are plotted. The resultant harmonic distortions K2, K3 and THD+N are computed as well and denoted in figure 5.

Because this software is an in-house development, it can be easily adapted for special cases and is therefore regularly used in the development process of electrodynamic transducers to find optimized designs. By using tools like this it is possible to get even closer to the physical limits.

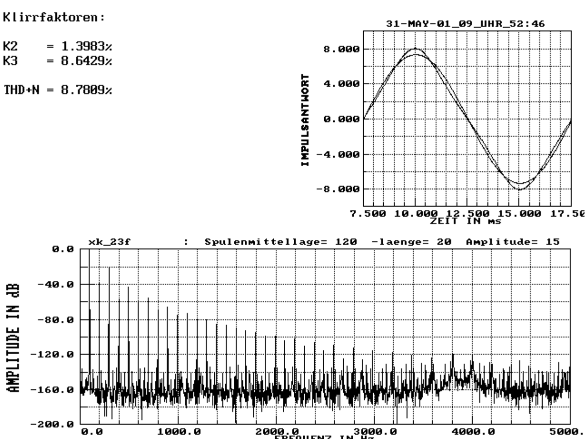

Fig. 5. Determination of harmonic distortion for a given voice coil position and amplitude of voice coil movement. Odd harmonics show a larger contribution than even harmonics.

MECHANO-ACOUSTICAL COMPUTATIONS

Finding an optimal shape of the membrane is an important step in the development process of a dynamic transducer. Up to the last decade, most of the research work was driven by measuring real-world prototypes. Though measuring is a very important part of the development process, there are some drawbacks. Measuring a real-world transducer prototype means to manufacture the membrane, assemble the transducer and carry out the measurements. This is a very time and cost consuming process. The Finite Element Method (FEM) and the Boundary Element Method (BEM) are two appropriate tools to calculate the behavior of membranes numerically [3]. FEM is a tool for solving the equation of motion. This is done by dividing a mechanical structure into elements with finite length. With BEM it is possible to couple the mechanical structure to the surrounding medium (i.e. air in our case). Here the acoustic wave equation based on Helmholtz’s equation has to be solved. But it is still advantageous to measure the real-world prototypes in order to verify the simulations. Only the combination of measuring and calculating the motion of membranes leads to optimized simulation models. A typical development process contains four different simulations, which are described in the following. After a short overview on the basic steps, the attention is turned to nonlinear and coupled FEM/BEM analysis.

Structural mechanics models

Here the FEM is used to compute eigenfrequencies and eigenmodes of some membranes in vacuum. Based on simplified construction drawings, finite element meshes using shell elements located at the midplane of the membrane are generated. A typical mesh is given in figure 6.

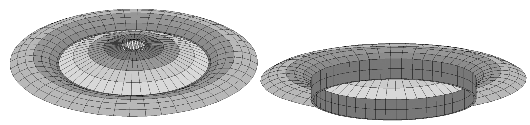

Fig. 6. Typical FEM mesh of a membrane with voice coil

The membrane itself as well as the voice coil are modeled. The appropriate material parameters, e.g. Young's modulus, are derived from some text books or are based on special measurements. Most of interest are the first few lower modes. Figure 7 shows typical mode shapes derived via finite element simulations.

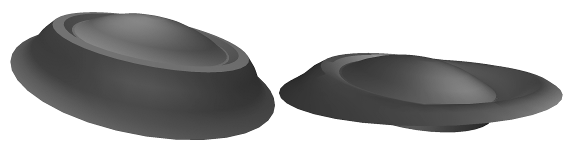

Fig. 7. Piston mode and rocking mode

The first mode shape, known as piston-mode, is primarily used for calibrating the FEM-model based on measurements of the main resonance in vacuum.

Forced response

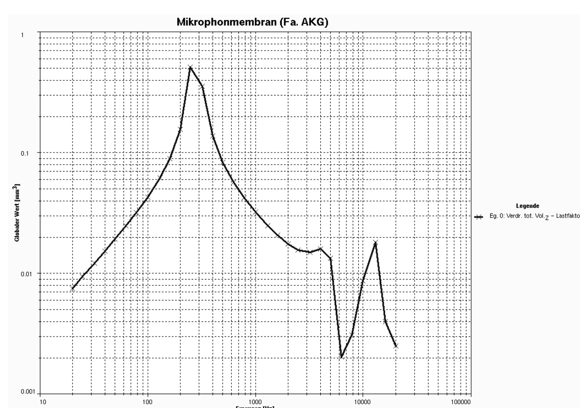

Fig. 8. Displaced volume vs. frequency

To calculate the behavior of the membrane in the frequency domain, the above presented model was extended by including mechanical forces acting at the voice coil. In this case the membrane acts like a loudspeaker. This model can be seen as a preliminary study for calculations using a fully coupled fluid-structure interaction model. Typically the displaced volume is used for the characterization of the membrane, like shown in figure 8.

Nonlinear static analysis

One of the goals in a typical design process nowadays is to “squeeze out the last dB’s”. So it is of importance to drive the membrane of loudspeakers with large excursions. However, measurements show that the acoustic quality is only acceptable up to a specific amplitude due to mechanical membrane behavior. Therefore a fully nonlinear static analysis is performed to calculate the nonlinear force-displacement behavior in both directions of a membrane. Figures 9 and 10 show the calculated results.

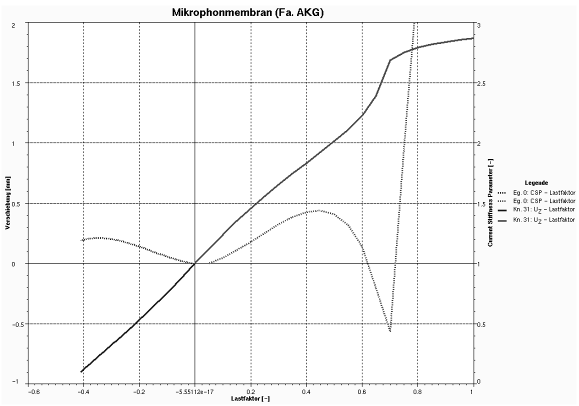

Fig. 9. Nonlinear force-displacement path and "Current Stiffness Parameter" for transducer membrane

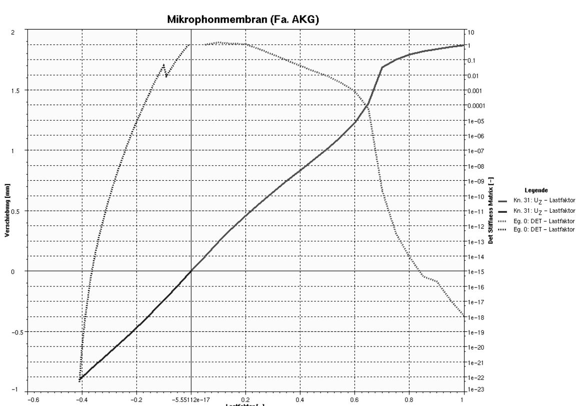

Fig. 10. Nonlinear force-displacement path and "Determinant of stiffness matrix" for transducer membrane

Due to the nonlinear behavior of the structure, stability points in both directions due to bifurcation and snap-through can be found. To detect these stability points, the "Current Stiffness Parameter" and the "Determinant Criteria" is used. Figures 9 and 10 correspondingly show the calculated path along the loading of the "Current Stiffness Parameter" and the "Determinant of the stiffness matrix". The bold lines represent the displacement, while the dotted lines correspond to the stiffness parameters.

The singularity of the “Current stiffness parameter” in figure 9 indicates bifurcation, like shown in figure 11. The steep decrease of the determinant in figure 10 for negative displacement indicates “snap-through”, like shown in figure 12. These effects set the limit for the maximum excursion of the transducer membrane.

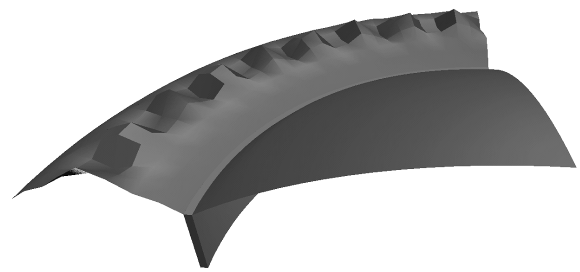

Fig. 11. Mode shape due to bifurcation

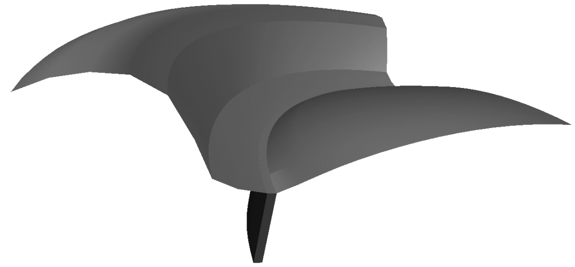

Fig. 12. Mode shape due to snap-through

Fluid-structure coupled analysis

The closest results to real-world behavior are delivered by simulations of membranes with respect to fully coupled fluid-structure interaction. Based on the presented simulation models a Boundary Element (BEM) mesh is added to the FEM mesh. This is necessary in order to solve the acoustic wave equation based on Helmholtz's equation. Figures 13 and 14 show a comparison of calculated and measured results. We see a good agreement throughout the frequency range of 100 Hz up to 20 kHz.

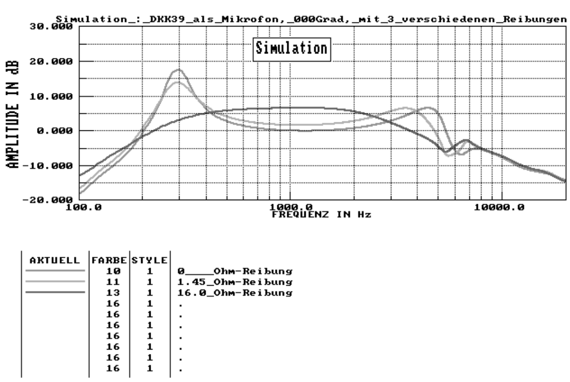

Fig. 13. Calculated results based on fully coupled fluid-structure interaction model

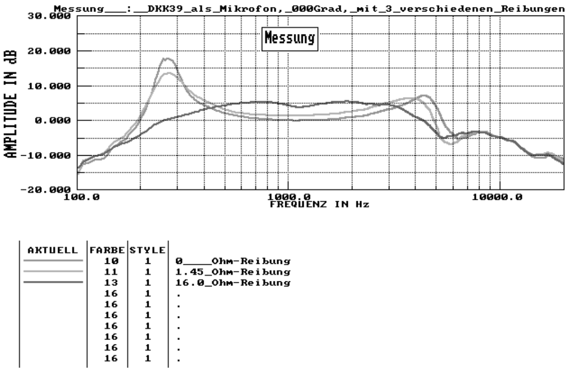

Fig. 14. Measured results

OPTICAL MEASUREMENTS

In order to verify the results of simulations and calculations, it is very useful to examine the real-world behavior of the transducer with a laser vibrometer. This is a computer controlled device which is able to measure the velocity of vibrating structures at predetermined positions.

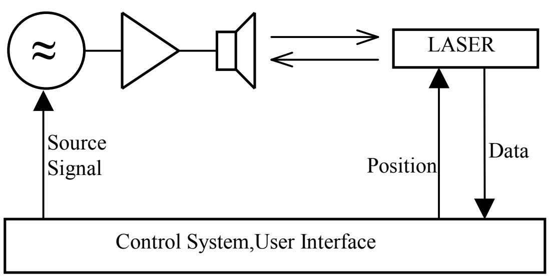

Fig. 15. Block diagram of the laser vibrometer

Although the laser vibrometer is a very powerful instrument, we will restrict our explanations only to those capabilities, which are advantageous for the analysis of dynamic transducers. The main principle is easy to understand. The transducer is excited with a selectable source signal, a laser beam measures the mechanical velocity at certain points upon the surface of the vibrating transducer, using the principle of laser-interferometry. The vibrometer is only capable of measuring the mechanical velocity. Displacement or acceleration have to be derived from the velocity information.

Before a measurement can be performed, certain measuring points have to be assigned. These points are positioned on a user-defined grid, which is projected at the observed structure. The amount of these points determines the mechanical resolution of the measurement. Examples of grids are shown in figure 16. During the measurement the transducer is scanned by the laser exactly at these points, one point after the other.

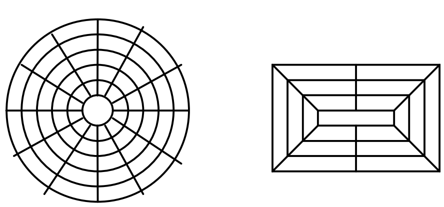

Fig. 16. Possible grids

Measuring the frequency response

After assigning a grid it is possible to analyze the frequency response. This is done by applying a signal containing all frequencies in the desired range to the transducer. Because the sound pressure level is proportional to the acceleration of the transducer, figure 17 shows the mean acceleration averaged over all grid points. This is a good approximation to the amplitude frequency response. It is also possible to observe the response of arbitrary points as well. This is shown in figure 18, where the displacement along four lines of intersection is displayed.

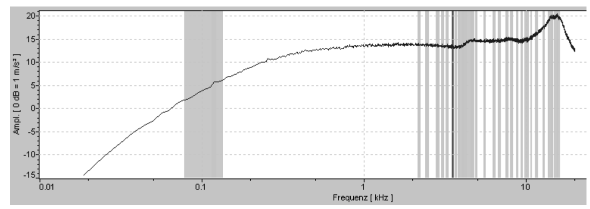

Fig. 17. Mean acceleration of a transducer surface

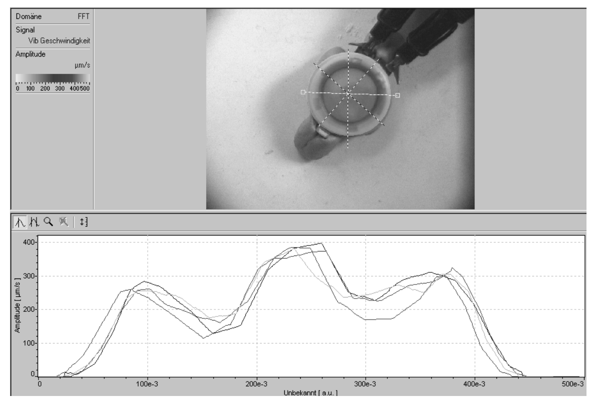

Fig. 18. Displacement along four lines of intersection

Modal analysis

In figure 17 some frequency ranges are marked as grey colums. By choosing a frequency it is possible to watch the behavior at this certain frequency. Peaks in the frequency response are auto-detected by the computer, the user is also authorized to designate certain ranges. Intensity peaks are very interesting for the acoustic designer, because they reveal (mostly unwanted) resonances. The two preferred methods to analyze those modes are “Isolines” and “3D”, as shown in figure 19. It is also possible to save the measurement as AVI-videofile to see the complete movement cycle.

In summary, the laser vibrometer helps to detect unwanted effects in the behavior of a transducer. When such an unwanted effect is identified during the development process, it is possible to counteract very efficiently.

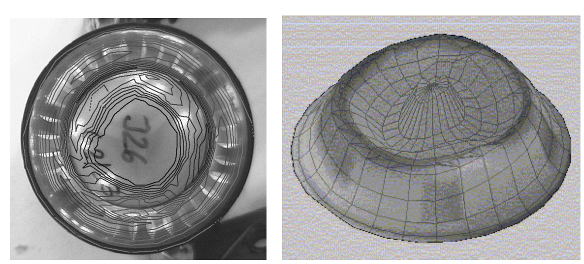

Fig. 19. Isolines and 3D diagram of a transducer mode

CONCLUSION

Three tools for the design process of electrodynamic tranducers were presented. Magnetic field computations, mechano-acoustical FEM/BEM calculations and laservibrometric measurements help the designer to predict and to analyze the behavior of the whole transducer or some parts of transducers. Due to these methods R&D costs can be further minimized, because models are built rather in the computer than in reality. In addition to this, numerical models allow to detect the influence of one single parameter only, which is hard to realize with a series of prototypes. A special focus was given on nonlinear effects when operated at high excursions. Although the simulations show a good approximation to the real-world behavior, it is a goal for the future work to combine these methods in a more efficient way. For example, the magnetic field computations could be considered in the boundary element simulations in order to get still closer to reality right from the beginning of each design process.

References

[1] Klippel, W. "Dynamic Measurement and Interpretation of Nonlinear Parameters of Electrodynamic Loudspeakers" J. AES, Vol 38, No. 12, December 1990

[2] Cermak, I., Silvester P. "Boundary-Relaxation Analysis of Rotationally Symmetric Electric Field Problems" IEEE Transaction on Power Apparatus and Systems, VOL. PAS-89, No. 5/6, May/June 1970

[3] Opitz, M., Svobodnik. A. "Elasto-acoustic simulations of microphone membranes" Proc. of NAFEMS-Seminar on Computational Acoustics, Wiesbaden, Germany, Nov 10-11, 1999